3rd European Conference on
Xylella fastidiosa and XF-ACTORS final meeting

A Model and Image based Investigation of *Xylella fastidiosa* Dynamics

Nancy Walker[1] (N.C.Walker@soton.ac.uk), Kathryn Rankin[2], Siul Ruiz[1], Daniel McKay Fletcher[1], Katherine Williams[1], Chiara Petroselli[1], Pasquale Salderelli[3], Maria Saponari[3], Steven White[4], and Tiina Roose[1]

1 Bioengineering Sciences Research Group, Department of Mechanical Engineering, School of Engineering, Faculty of Engineering and Physical Sciences, University of Southampton, UK

2 μ-VIS X-ray Imaging Centre, Faculty of Engineering and Physical Sciences, University of Southampton, UK

3 Istituto per la Protezione Sostenibile delle Piante, CNR, Bari, Italy

4 UK Centre for Ecology & Hydrology, Maclean Building, Benson Lane, Crowmarsh Gifford, Wallingford, Oxfordshire, UK

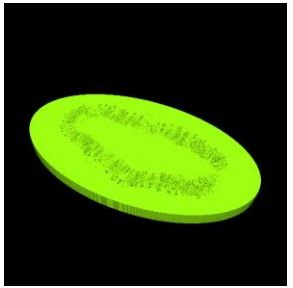

MOTIVATION AND OBJECTIVES

MOTIVATION

- *X. fastidiosa* has resulted in the devastation of several important commercial crops (Figure 1).
- Current modelling work focuses on limiting geographic spread.
- Studies that focus on physiological issues lack fundamental details.
- Elucidating these mechanistic causes of plant dieback can help to better understand causes of symptom expression and mechanisms of resistant hosts.

Figure 1: A photo depicting olive decline in Apulia, Dr Steven White

RESEARCH AIMS

Hypothesis: Differences in xylem geometry contribute to reduce the impact of *X. fastidiosa* biofilm development on hydraulic conductivity in resistant (Leccino and FS17) compared with susceptible (Ogliarola and Koroneiki) olive cultivars.

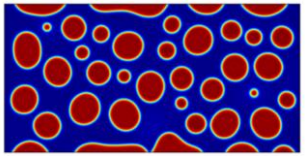

Figure 2: Biofilm Aggregation

Simulation of Cahn-Hilliard model equations, biofilm (red) collects into droplets that aggregate together and to the top and bottom surfaces. Droplets are suspended in surrounding water (blue).

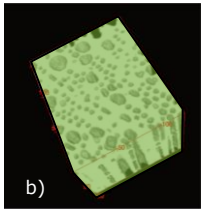

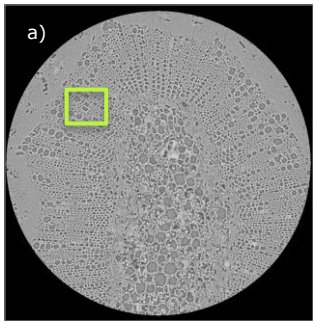

Figure 3: 3D Visualisation of Olive Cultivar Xylem Tissue Networks

A section of Ogliarola xylem tissue is highlighted in a 3D greyscale CT image stack (a). Vessels in this tissue create a porous network (b), that transports water through the plant.

- A biofilm model will be developed to describe *X. fastidiosa* formation and organisation (Figure 2) on CT geometries.
- 3D X-ray CT imaging (Figure 3) will be used to measure differences in aspects of xylem geometry between resistant and susceptible cultivars.

METHODS

XCT IMAGING

X-ray Computed Tomography (XCT): used to visualise xylem vessels. Scans capture 2mm^3 from samples of young stem (approx. 2mm diameter) at 1µm resolution.

- Xylem networks of resistant (Leccino, FS17) and susceptible (Ogliarola, Koroneiki) cultivars analysed using bespoke workflow (Figure 3).
- We quantify porosity, connectivity, and radii distributions.
- Obtained xylem networks will also aid model parametrisation and will form the spatial domain for simulations.

Figure 3: Image Analysis Workflow

Greyscale image stacks (a) are filtered before being segmented using a threshold. From the resulting binarised stacks (b), measurements are made, including the number of vessels (c), vessel length, vessel diameters (d), and vessel connections. Processing and measurements are carried out using Image J before being analysed in Python.

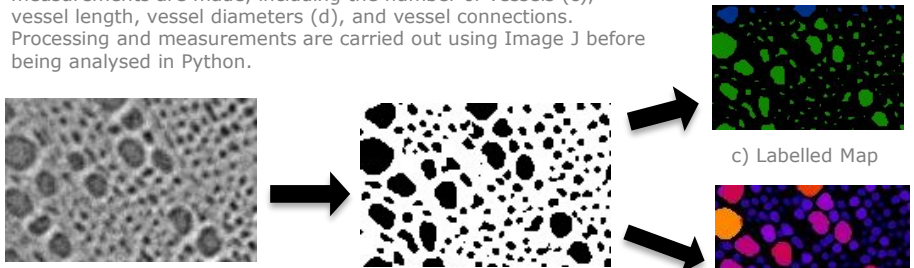

a) Greyscale Image

b) Binarised Image

c) Labelled Map

d) Thickness Map

MATHEMATICAL MODEL

- Biofilm – bacteria enclosed in extracellular polymeric substance (EPS) molecules - dominant component in determining 3D structure.
- Thus, we approximate the biofilm as a water-polymer mixture, capturing biofilm structure based on physiochemical first principles (Figure 4).

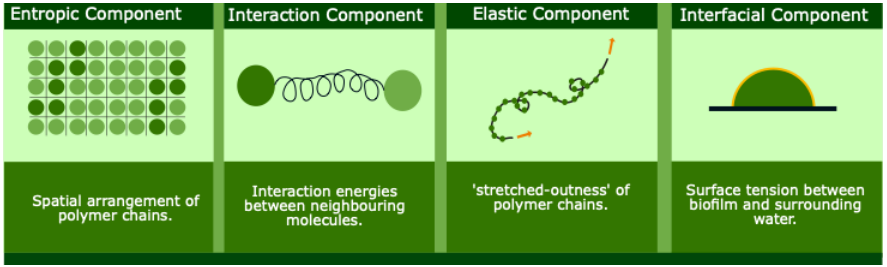

Figure 4: Physiochemical Components of Hydrogels

The model approximates the biofilm as a water-polymer mixture (hydrogel). In accordance with Flory theory, hydrogels consist of three free energy components; an entropic component, interaction component and elastic component. An interfacial component captures the surface tension between the biofilm and external xylem sap.

$$\textbf{1}\quad \partial_t \phi + \nabla \cdot \left(\phi \left[\boldsymbol{u} - \frac{\phi(1-\phi)^2}{\zeta} \nabla \mu \right] \right) = s \qquad \textbf{3}\quad \nabla \cdot \eta \nabla \boldsymbol{u} - \nabla p = \phi \nabla \mu$$

$$\textbf{2}\quad \mu = \partial_\phi f - \kappa \nabla^2 \phi \qquad \textbf{4}\quad -\nabla \cdot \boldsymbol{u} = 0$$

Model Equations – result from the assumptions by invoking Onsager's Principle :

1. Biofilm phase conservation equation – describes transport and formation of biofilm phase (ϕ)
2. Biofilm chemical potential (μ) – Energetic description of how biofilm spatially organises (f, κ)
3. Stokes flow – Momentum of bulk fluid flow ($\boldsymbol{u}$) considering chemical (μ) and pressure (p) potentials
4. Divergence free – Implies a balance between mass conservation

PRELIMINARY RESULTS AND OUTLOOK: CT MEASUREMENTS

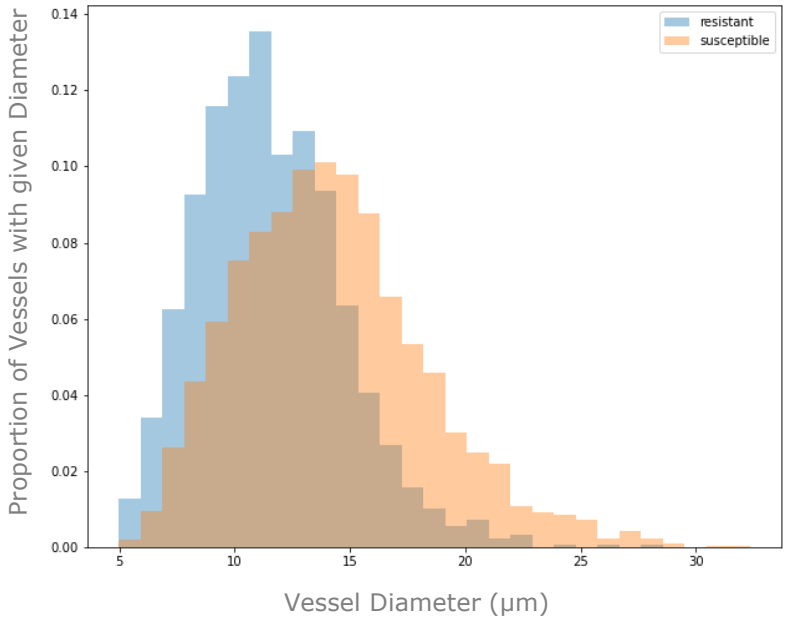

Preliminary Results:

- T-tests suggest that hosts of the 2 different resistant ($p = 0.231$, 3 s.f.), and respectively susceptible ($p = 0.171$, 3 s.f.) cultivars have similar mean vessel diameter.
- Histograms (Figure 5) suggest that vessels of resistant cultivars Leccino and FS17 have on average smaller, and more similar diameter than those of susceptible cultivars Ogliarola and Koroneiki.

Outlook:

- Carry out more statistical tests on diameter measurements.
- Correlate vessel diameter measurements to hydraulic conductivity.
- Investigate other morphological features between resistant and susceptible cultivars.

Figure 5: Histogram Comparing Vessel Diameters in Resistant and Susceptible Olive Cultivars

A histogram shows, in blue, the distribution of average xylem vessel diameters collectively from 3 samples of each of 2 resistant olive cultivars (Leccino and FS17), and in orange, that of those from 3 samples of each of 2 susceptible olive cultivars (Ogliarola and Koroneiki). T-tests were carried out to ensure means between the two resistant (respectively, the two susceptible) cultivars were not significantly different. The plot suggests that cultivars Ogliarola and Koroneiki have vessels with on average larger, and more variable diameters than those of cultivars Leccino and FS17, though statistical tests are needed to confirm the significance of this observation.

PRELIMINARY RESULTS AND OUTLOOK: BIOFILM MODEL

ORGANISATION

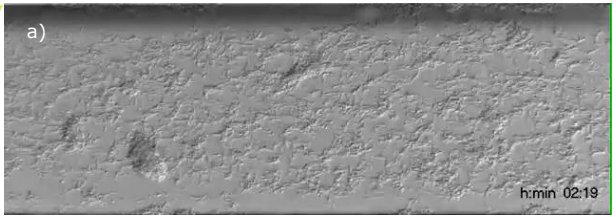

GROWTH

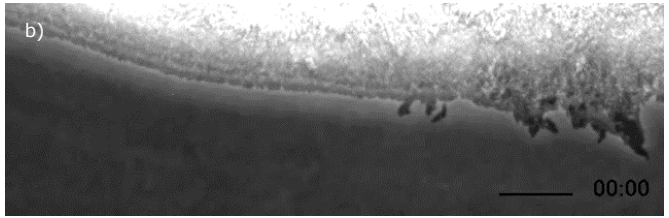

http://web.ppmb.cals.cornell.edu/huch/movies/ (accessed 17/04/21) - movies of *X.fastidiosa* aggregation/organisation (a) and growth (b), link courtesy of Professor Leonardo de la Fuente

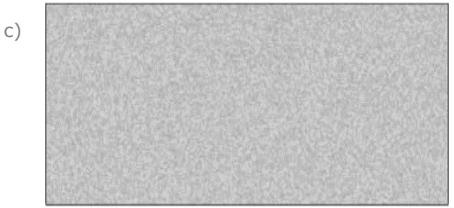

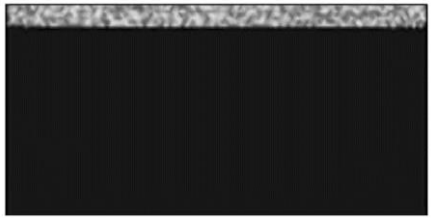

Corresponding simulations of model equations 1 and 2 carried out in COMSOL Multiphysics 5.5, capturing analogous patterns of organisation (c) and growth (d).

Figure 6: X.fastidiosa Organisation and Growth - Comparing Model Simulations to Experiments

Movies showing *X.fastidiosa* b) colony expansion and a) aggregation in a microfabricated fluidic chamber are compared with corresponding simulations. Simulations of Cahn Hilliard (equations 1 and 2) model equations were carried out with a random initial condition (representative of experimental flushing) and zero source term to capture organisation and aggregation (c), and a random initial condition within a thin layer (bacteria initialised on a surface) and non zero source term to capture surface droplet formation and growth.

Preliminary Results:

- Model simulations are able to capture spatial organisation with just the polymer physics (Figure 6).

Outlook:

- Accurate parametrisation of growth source term is required to capture growth with correct time scales.
- The model will later be applied to XCT-based geometries from susceptible and resistant olive cultivars to capture any differences in disease development.